

Received XX Month, XXXX; revised XX Month, XXXX; accepted XX Month, XXXX; Date of publication XX Month, XXXX; date of current version XX Month, XXXX.

Digital Object Identifier 10.1109/OJCOMS.2022.1234567

NOMA Made Practical: Removing the Receive SIC Processing through Interference Exploitation

Abdelhamid Salem^{1,2}, Member, IEEE, Xiao Tong³, Ang Li³, Member, IEEE, and Christos Masouros¹ Fellow, IEEE

¹Department of Electronic and Electrical Engineering, University College London, London, UK.

²Department of Electronic and Electrical Engineering, Benghazi University, Benghazi, Libya.

³School of Information and Communications Engineering, Xi'an Jiaotong University, Xi'an, Shaanxi 710049, China.

CORRESPONDING AUTHORS: Abdelhamid Salem (e-mail: a.salem@ucl.ac.uk).

This work is supported by the U.K. Engineering and Physical Sciences Research Council (EPSRC) under grant EP/W026252/1.

ABSTRACT Non-orthogonal multiple access (NOMA) is a powerful transmission technique that enhances the spectral efficiency of communication links, and is being investigated for 5G standards and beyond. A major drawback of NOMA is the need to apply successive interference cancellation (SIC) at the receiver on a symbol-by-symbol basis, which limits its practicality. To circumvent this, in this paper a novel constructive multiple access (CoMA) scheme is proposed and investigated. CoMA aligns the superimposed signals to the different users constructively to the signal of interest. Since the superimposed signal aligns with the data signal, there is no need to remove it at the receiver using SIC. Accordingly, SIC component can be removed at the receiver side. In this regard and in order to provide a comprehensive investigation and comparison, different optimization problems for user pairing NOMA multiple-input-single-output (MISO) systems are considered. Firstly, an optimal precoder to minimize the total transmission power for CoMA subject to a quality-of-service constraint is obtained, and compared to conventional NOMA. Then, a precoder that minimizes the CoMA symbol error rate (SER) subject to power constraint is investigated. Further, the computational complexity of CoMA is considered and compared with conventional NOMA scheme in terms of total number of complex operations. The results in this paper prove the superiority of the proposed CoMA scheme over the conventional NOMA technique, and demonstrate that CoMA is an attractive solution for user pairing NOMA MISO systems with low number of BS antennas, while circumventing the receive SIC complexity.

INDEX TERMS NOMA, constructive interference, successive interference cancellation.

I. Introduction

Non-orthogonal multiple access (NOMA) technique has received significant attention very recently as a viable multiple access technique for communication networks [1]. In NOMA the transmitter superimposes the users signals in same frequency, time, and code domains while being able to resolve the signals in the power domain. In conventional NOMA, the users with poor channel conditions (weak users) detect their signals by treating the other users' signals as noise. On the contrary, the users with strong channel conditions (strong users) first decode the signals of the weak users, then they detect their own signals

by removing the weak users' signals using successive interference cancellation (SIC) [1]. This is a significant known limitation of NOMA, which poses impractical symbol-by-symbol complexity. The efficiency of NOMA technique has been extensively investigated in the literature. For instance, the results in [2] showed that NOMA can achieve superior performance comparing with orthogonal multiple access (OMA) schemes. The performance of NOMA was analyzed in [3] based on the availability of the channel state information (CSI) at the transmitter. In [4] a power minimization problem for two-users multiple-input-single-output (MISO)-NOMA systems was formulated and

solved. The results in this work showed that the proposed NOMA approach can enhance the performance of MISO systems. To maximize the fairness among the users in NOMA systems, an optimal power allocation scheme has been considered in [5].

Furthermore, in NOMA systems when number of users is large, the interference in the system might be strong. This interference will lead to increase the complexity and the processing delay at the receivers. More relevant to this work, in order to reduce the interference, complexity and processing delay, user pairing scheme has been proposed and considered in the literature [6]–[9]. In this scheme, each two users (pair) share a specific orthogonal resource slot and NOMA technique is implemented among the users in each pair. User pairing scheme has been widely investigated in the literature. The authors in [7] proposed a user pairing scheme in which the network area is divided into two regions, near and far regions, and each far user is paired with a near user. The results in [7] explained that, the performance gain performed by NOMA over OMA can be further improved by pairing the users whose channel conditions are more distinctive. In [8] MU-MIMO NOMA systems was considered, in which the users are paired and share the same transmit beam-forming vector. Under this scenario, the superiority of MIMO-NOMA over MIMO-OMA has been proved for a two-user pairing scenario. The authors in [9] proposed a greedy-search based user pairing scheme in order to maximize the achievable sum rate of NOMA system.

In parallel, constructive interference (CI) precoding has received research interest in the last few years [10]–[13]. CI precoding is also a non-orthogonal transmission approach which exploits the known interference to improve the system performance. Based on the knowledge of the CSI and the users messages, the BS can classify the multi-user interference as constructive and destructive. The constructive interference can be defined as the interference that can move the received symbol deeper in the detection region of the constellation point of interest. Accordingly, a constructive precoder can be obtained to make the known interference in the system constructive to the received symbols. The CI concept has been widely studied and investigated in the literature. This line of research introduced in [10], where the CI precoding technique has been proposed for downlink MIMO systems, showing significant performance improvements over conventional precoding. The first optimization based CI approach was introduced in [11] where a modified vector-perturbation technique was proposed, in which the search of perturbing vectors was limited to a specific area where the distances from the decision thresholds are increased with respect to a distance threshold. In [12], the authors used the concept of CI to exploit the known interference as green signal energy for downlink transmission. By doing so, the transmit power can be reduced, and thus enhancing the power

efficiency of transmission. Further work in [14], [15], a general category of CI regions has been considered, and the features of this region have been studied. Different convex alphabet relaxation schemes for vector precoding in MIMO broadcast channels have been proposed in [16] to achieve interference-free communication over singular channels. It has been shown in [17] that vector precoding can be implemented to reduce the transmission power of MIMO systems. The authors in [18] implemented CI precoding scheme in wireless power transfer scenarios to minimize the total transmit power. In [19] a CI optimization problem to minimize a sum of minimum mean square error for all users has been considered. Novel strategies that exploit the potential of CI precoding to control the per-antenna transmit power has been presented in [20]. The authors in [21] addressed the robust design problem of CI precoding transmission scheme in a multiple-users MISO (MU-MISO) system. Recently in [22], [23] closed-form expressions of CI precoding scheme for phase-shift keying (PSK) and quadrature amplitude modulation (QAM) have been derived. These expressions have derived based on optimal performance, thus its performance is equivalent to the optimization-based CI schemes presented in the literature. Based on these closed form expressions, in our previous works in [24] analytical expressions of the achievable sum-rate of CI precoding have been derived for different scenarios. For more details, the reader is referred to [25] where the concept of the CI precoding scheme and its practical implementation have been presented and discussed in details¹.

Very recently, there has been a tremendous effort regarding pushing the frontier of NOMA. For instance, in [26] a simple scheme was proposed to reduce the detection complexity of NOMA receivers. In this scheme, the input distributions were deliberately chosen to be uniformly distributed over some pulse amplitude modulations (PAM) such that the decoder can treat the interference as noise without degrading the performance. The authors in [27] generalized the scheme in [26] to a general lattice partition framework for downlink NOMA systems without SIC by employing two-steps. In the first step, the corresponding linear deterministic model was investigated and an optimal input distribution was derived. This optimal distribution was then translated into a uniform distribution over a properly chosen PAM constellations. Further work in [28] developed a lattice-partition-based downlink NOMA scheme which adopts discrete inputs according to statistical CSI. In [29] the authors proposed a loss-less NOMA implementation without SIC, this implementation was achieved via correlated a superposition coding.

¹Note that, dirty-paper coding is difficult to implement in practical systems, due to the impractical assumption of infinite codewords length and its very high computational cost. Therefore, precoding schemes with lower complexity such as CI have received increasing research attention.

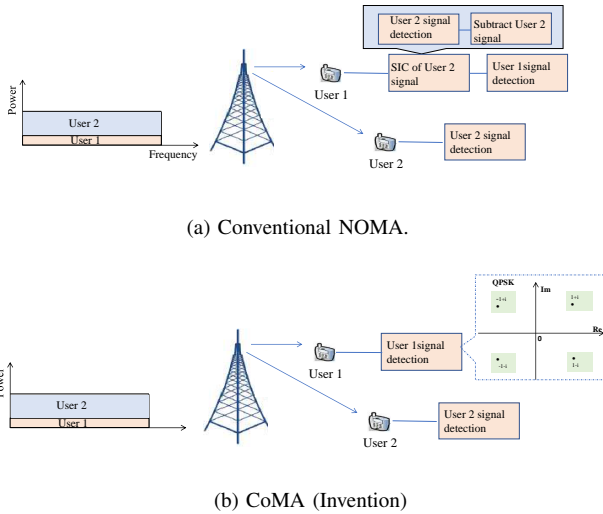


FIGURE 1. Conventional NOMA and CoMA schemes.

In line with the previous works, in this paper we exploit the CI concept to address a major limitation of NOMA systems. This is the need to apply SIC on a symbol-by-symbol basis at the receiver, which introduces impractical complexity. Accordingly, we propose an approach to entirely circumvent SIC, based on the concept of CI. We introduce a new constructive multiple access NOMA (CoMA) precoding technique that aligns the superimposed signals to the different user equipments (UE) constructively to the signal of interest. The key principle is shown in Fig. 1b, contrasting it with the classical NOMA approach in Fig. 1a. Since for CoMA the superimposed signal aligns with the data signal, the received symbol appears at the correct constellation region, it does not require channel equalization and there is no need to remove the interfering symbol at the strong user receiver using SIC technique. Critically, this new scheme allows the following key gains that make NOMA practical:

- 1) A low complexity UE - by removing SIC from the receiver, CoMA allows minimal receive signal processing as shown in Fig. 1b.
- 2) Since channel equalization is not required, this removes the need for channel state information (CSI) at the strong UE [25].
- 3) Reduces the latency in processing the received signal on a symbol-by-symbols basis at the UE.
- 4) The interference contributes constructively to the useful signal, and this leads to increase received signal power.
- 5) CoMA can be used with any finite-alphabet signals.

Due to the above key advantages, the proposed approach makes NOMA more practical and fits different practical scenarios. In this regard and in order to provide a comprehensive comparison, based on the CoMA concept, two new optimal precoders are designed, one to minimize the total transmit power and one to minimize the symbol

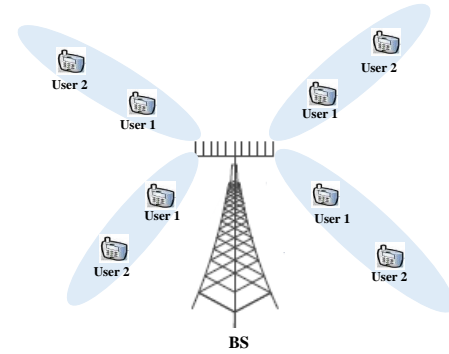


FIGURE 2. A multiuser NOMA system with K pairs.

error rate (SER) for a given NOMA pair. In addition, the receiver complexity of CoMA scheme is investigated and compared with conventional NOMA scheme.

For clarity we highlight the main contributions of this work as follows.

- 1) CoMA scheme is proposed and introduced for the first time to remove receive SIC and reduce the complexity of user pairing NOMA MISO systems.
- 2) New CoMA precoder that minimizes the transmit power for a given system performance is designed.
- 3) We further adapt CoMA concept to design new precoder that is able to minimize the system error rate subject to total power constraint.
- 4) The complexity analysis of the proposed CoMA scheme is considered and investigated.
- 5) The performance of CoMA scheme is compared with OMA and conventional NOMA precoders.

The results in this work show that CoMA scheme consumes much less power than conventional NOMA and OMA techniques to achieve similar target rates. In addition, CoMA scheme has lower error rate than OMA and conventional NOMA schemes. Furthermore, our results confirm that the new proposed CoMA scheme has very low computational receiver complexity compared to conventional NOMA technique².

II. System Model

We consider a down-link MU-MISO system, in which a BS equipped with N antennas transmits information signals to $2K$ single antenna users using user-pairing NOMA technique [6]–[9]. In this system, each two users are paired to form a cluster, and hence, there are K pairs/clusters in the system as shown in Fig. 2. Block fading channel model is assumed, in which each channel coefficient includes both small scale fading and large scale fading. The $N \times 1$ channel vector between the BS and user i , $i \in \{1, 2\}$ in pair k , $k \in \{1, \dots, K\}$, is $\mathbf{h}_{k,i} \sim \mathcal{CN}(0, \mathbf{I}_N \sigma_{k,i}^2)$.

²Parts of this paper were presented at the ISWCS 2022 [30].

Following the principle of NOMA, the BS broadcasts a superimposed message of the two users in each pair. For pair k , the BS transmits $\mathbf{x}_k = \mathbf{w}_{k,1}x_{k,1} + \mathbf{w}_{k,2}x_{k,2}$, where $x_{k,1}$ and $x_{k,2}$ are the data symbols for user 1 ($u_{k,1}$) and user 2 ($u_{k,2}$) with unit variance, $\mathbf{w}_{k,i}$ is the precoding vector of user i . In user-pairing NOMA scheme the two users in each pair are ordered based on their CSI. Without loss of generality, user 1, is assumed to have a better channel than user 2³. The received signals at user 1 and user 2 in pair k can be written as

$$y_{u_{k,i}} = \mathbf{h}_{k,i}^T \sum_{l=1}^2 \mathbf{w}_{k,l} x_{k,l} + n_{u_{k,i}}, \quad (1)$$

where $n_{u_{k,i}}$ is the additive white Gaussian noise (AWGN) at user i with variance $\sigma_{u_{k,i}}^2$, $n_{u_{k,i}} \sim \mathcal{CN}(0, \sigma_{u_{k,i}}^2)$. Based on NOMA, the stronger user, user 1, adopts a SIC, in which user 1 first detects user 2 signal, and then removes the detected signal term from the received signal to decode its own message. Thus, the received SINR at user 1 to detect user 2 signal, $x_{k,2}$, can be written as,

$$\gamma_{x_{k,2} \rightarrow u_{k,1}} = \frac{|\mathbf{h}_{k,1}^T \mathbf{w}_{k,2}|^2}{|\mathbf{h}_{k,1}^T \mathbf{w}_{k,1}|^2 + \sigma_{u_{k,1}}^2}, \quad (2)$$

The data rate for user 1 to detect user 2 signal, $R_{x_{k,2} \rightarrow u_{k,1}}$, should be larger than the target rate of user 2 and thus $\gamma_{x_{k,2} \rightarrow u_{k,1}}$ should be higher than the target SINR at user 2 (r_2). The received signal at user 1 after using SIC is given by

$$y_{u_{k,1}} = \mathbf{h}_{k,1}^T \mathbf{w}_{k,1} x_{k,1} + \epsilon + n_{u_{k,1}}, \quad (3)$$

where ϵ is the SIC error with variance σ_ϵ^2 . This error may occur due to incorrect detection of $x_{k,2}$, incorrect CSI knowledge, or incorrect knowledge of the power allocation at the BS.

Consequently, the received SINR at user 1 and user 2, to detect $x_{k,1}$ and $x_{k,2}$, respectively, can be written as

$$\gamma_{u_{k,1}} = \frac{|\mathbf{h}_{k,1}^T \mathbf{w}_{k,1}|^2}{\sigma_\epsilon^2 + \sigma_{u_{k,1}}^2}, \quad (4)$$

$$\gamma_{u_{k,2}} = \frac{|\mathbf{h}_{k,2}^T \mathbf{w}_{k,2}|^2}{|\mathbf{h}_{k,2}^T \mathbf{w}_{k,1}|^2 + \sigma_{u_{k,2}}^2}. \quad (5)$$

However, as we have explained earlier, NOMA scheme suffers from a key challenge. The need to perform SIC at the receiver on a symbol-by-symbol level, i.e. for an LTE frame on the order of 0.1msec. This implicates:

- Large complexity at the UE receiver that makes the practical application challenging.

³The optimal power allocation between the users depends on quality of service (QoS) requirements [31].

- Increased latency in the signal detection.
- Overheads in obtaining/feedback of CSI.
- Increased transmit power when the SIC errors increase.

In order to overcome all these challenging points CoMA technique is proposed and presented in the next Section.

To evaluate the complexity gains of our approach, we chose to compare to the least-complexity NOMA where we consider SIC at the symbol level. CoMA scheme can be applied also for block level SIC. It is also worth mentioning that, symbol-based SIC suffers from severe error propagation without coding. Thus, to reduce the impact of symbol-level error propagation in conventional NOMA, coding techniques can be employed. Error-correcting codes allow the receiver to detect and correct errors that occur during symbol-level processing and decoding [32].

III. Constructive NOMA (CoMA) Scheme

The main idea of CoMA scheme is to align the superimposed signals that is known to the BS to increase the useful signal power at the receiver. As we mentioned earlier, the interference signal is constructive if it can move the received symbol towards the detection/constructive region. The basic concept of CI precoding for QPSK constellation is summarized in Fig. 3. Without loss of the generality, we denote $\vec{OA} = t.s_{u_1}$ as the scaled data symbol, and $t = \sqrt{\Gamma_{u_{k,1}} \sigma_{u_{k,1}}^2}$ corresponds to our considered QPSK modulation, where $\Gamma_{u_{k,1}}$ is the SNR target for user 1 [25]. When $|\vec{CD}| \geq |\vec{CB}|$ is satisfied, the interference signal is constructive and moves the received symbol towards the detection/constructive region. Based on the Fig. 3, we know that $|\vec{CB}| = |\mathcal{J}(y_{u_{k,1}})|$ and $|\vec{CA}| = |\vec{OC}| - |\vec{OA}|$, where $|\vec{OA}| = \sqrt{\Gamma_{u_{k,1}} \sigma_{u_{k,1}}^2} = \sqrt{SNR_{u_{k,1}} \sigma_{u_{k,1}}^2}$, so $|\vec{CD}|$ can be expressed as $|\vec{CD}| = |\vec{AC}| \cdot \tan \theta_t = [\mathcal{R}(y_{u_{k,1}}) - \sqrt{SNR_{u_{k,1}} \sigma_{u_{k,1}}^2}] \cdot \tan \theta_t$. Following this derivation, we can write the CI constraint as

$$|\vec{CD}| \geq |\vec{CB}|$$

$$\Rightarrow [\mathcal{R}(y_{u_{k,1}}) - \sqrt{SNR_{u_1} \sigma_{u_1}^2}] \cdot \tan \theta_t \geq |\mathcal{J}(y_{u_{k,1}})| \quad (6)$$

Additionally, the constructive areas for BPSK, QPSK, 8PSK and 16 QAM are shown in Fig. 4. For more details, the reader is referred to [25] where the interference exploitation scheme has been discussed and the practical implementation of CI precoding has been presented.

Therefore, following the CI principle [25] the transmit precoding can be designed to impose constructive interference to the desired symbol. When the interference is aligned by means of precoding vectors to overlap constructively with the signal of interest, all interference

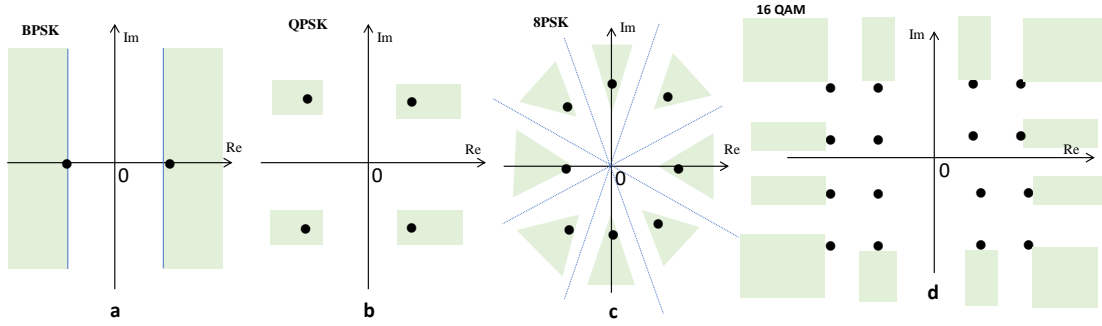


FIGURE 4. Constructive interference in a) BPSK, b) QPSK, c) 8PSK, and d) 16 QAM the constructive regions are represented by the green areas.

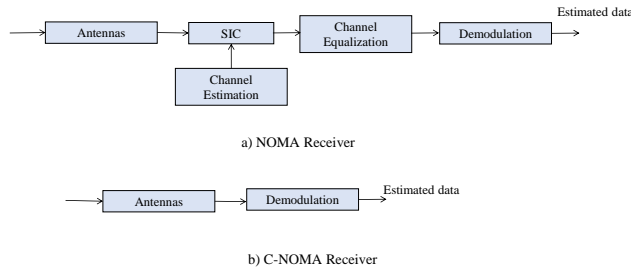


FIGURE 5. Receivers of conventional and constructive NOMA schemes.

$$\begin{aligned} & \min_{\mathbf{w}_i \succeq \mathbf{0}} \left\| \sum_{i=1}^2 \mathbf{w}_i e^{j(\phi_i - \phi_1)} \right\|^2 \\ & \text{s.t. } \mathbf{C1} : \left| \text{Im} \left(\mathbf{h}_1^T \sum_{k=1}^2 \mathbf{w}_k e^{j(\phi_k - \phi_1)} \right) \right| \leq \\ & \quad \left(\text{Re} \left(\mathbf{h}_1^T \sum_{k=1}^2 \mathbf{w}_k e^{j(\phi_k - \phi_1)} \right) - \sqrt{r_1 \sigma_{u_1}^2} \right) \tan \theta \\ & \mathbf{C2} : 2\text{Re}(\bar{\mathbf{w}}_2^H \mathbf{h}_2 \mathbf{h}_2^T \mathbf{w}_2) - \text{Re}(\bar{\mathbf{w}}_2^H \mathbf{h}_2 \mathbf{h}_2^T \bar{\mathbf{w}}_2) \geq \\ & r_2 (2\text{Re}(\bar{\mathbf{w}}_1^H \mathbf{h}_2 \mathbf{h}_2^T \mathbf{w}_1) - \text{Re}(\bar{\mathbf{w}}_1^H \mathbf{h}_2 \mathbf{h}_2^T \bar{\mathbf{w}}_1)) + \sigma_{u_2}^2 r_2 \end{aligned} \quad (13)$$

Finally, the all steps to solve (13) and find the optimal precoding vectors using first-order Taylor expansion method is presented in Algorithm 1.

B. Review: Conventional NOMA Precoding

The total power consumption in conventional NOMA is $P = \sum_{i=1}^2 \|\mathbf{w}_i\|^2$. Consequently, from (2), (4) and (5) the power minimization problem can be formulated as

Algorithm 1 Iterative Algorithm for (13).

- 1: Set the maximum number of iterations Q .
- 2: Randomly generate $\bar{\mathbf{w}}_i$.
- 3: Repeat
- 4: Using CVX to solve (13) as \mathbf{w}_i^* .
- 5: Update $\bar{\mathbf{w}}_i = \mathbf{w}_i^*$
- 6: $q = q + 1$.
- 7: Until $q = Q$.
- 8: Output \mathbf{w}_i^* , $i \in K$.

$$\begin{aligned} & \min_{\mathbf{w}_i} \sum_{i=1}^2 \|\mathbf{w}_i\|^2 \\ & \text{s.t. } \mathbf{C1} : \gamma_{u_1} \geq r_1 \\ & \quad \mathbf{C2} : \gamma_{u_2} \geq r_2 \\ & \quad \mathbf{C3} : \gamma_{x_2 \rightarrow u_1} \geq r_2 \end{aligned} \quad (14)$$

The constraint **C3** to ensure the successful SIC for the strong user. The last expression in (14) can be presented in more detailed formula as

$$\begin{aligned} & \min_{\mathbf{w}_i} \sum_{i=1}^2 \|\mathbf{w}_i\|^2 \\ & \text{s.t. } \mathbf{C1} : |\mathbf{h}_1^T \mathbf{w}_1|^2 \geq (\sigma_\epsilon^2 + \sigma_{u_1}^2) r_1 \\ & \quad \mathbf{C2} : |\mathbf{h}_2^T \mathbf{w}_2|^2 \geq (|\mathbf{h}_2^T \mathbf{w}_1|^2 + \sigma_{u_2}^2) r_2 \\ & \quad \mathbf{C3} : |\mathbf{h}_1^T \mathbf{w}_2|^2 \geq (|\mathbf{h}_1^T \mathbf{w}_1|^2 + \sigma_{u_1}^2) r_2 \end{aligned} \quad (15)$$

Semidefinite relaxation (SDR) can be used to obtain the optimal precoders in (15). The effectiveness of the SDR to solve this transmit beamforming problem has been widely considered in literature [35], [36]. The problem in (15) has been investigated and considered in details in [4], where the optimal and closed form solutions have been provided.

V. SER Minimization

In this Section we design precoder vectors to minimize the SER subject to total transmission power constraint. For sake of comparison, CoMA and NOMA are considered in this Section.

A. CoMA Precoding

In this Section we consider SER for the proposed CoMA scheme. To minimize the SER of the proposed CoMA scheme, we construct the following optimization problem:

$$\begin{aligned} \mathcal{P}_1 : & \min_{\mathbf{w}_1, \mathbf{w}_2} \max_k \{\text{SER}_k\} \\ \text{s.t. C1:} & \left\| \sum_{k=1}^2 \mathbf{w}_k e^{j(\phi_k - \phi_1)} \right\|^2 < P \\ \text{C2:} & \left| \text{Im} \left(\mathbf{h}_1^T \sum_{k=1}^2 \mathbf{w}_k e^{j(\phi_k - \phi_1)} \right) \right| \leq \\ & \left(\text{Re} \left(\mathbf{h}_1^T \sum_{k=1}^2 \mathbf{w}_k e^{j(\phi_k - \phi_1)} \right) - \sqrt{\text{SNR}_1 \sigma_{u1}^2} \right) \tan \theta_t \end{aligned} \quad (16)$$

where P is the total transmit power, **C1** represents the total transmit power budget and **C2** represents the constructive interference constraint for user 1, respectively. According to the monotonicity that the SER decreases with the increase of the received SNR, we transform the original optimization problem into the following form:

$$\begin{aligned} \mathcal{P}_2 : & \max_{\mathbf{w}_1, \mathbf{w}_2} \min_k \{\text{SNR}_k\} \\ \text{s.t. C1:} & \left\| \sum_{k=1}^2 \mathbf{w}_k e^{j(\phi_k - \phi_1)} \right\|^2 < P \\ \text{C2:} & \left| \text{Im} \left(\mathbf{h}_1^T \sum_{k=1}^2 \mathbf{w}_k e^{j(\phi_k - \phi_1)} \right) \right| \leq \\ & \left(\text{Re} \left(\mathbf{h}_1^T \sum_{k=1}^2 \mathbf{w}_k e^{j(\phi_k - \phi_1)} \right) - \right. \\ & \left. |(\mathbf{h}_1^T (\mathbf{w}_1 e^{j\phi_1} + \mathbf{w}_2 e^{j\phi_2}))| \right) \tan \theta_t \\ \text{C3:} & \text{Im}(\mathbf{h}_2^T \mathbf{w}_2) = 0, \text{Re}(\mathbf{h}_2^T \mathbf{w}_2) \geq 0 \end{aligned} \quad (17)$$

where the additional constraint **C3** can guarantee that the received symbol for user 2 lies in the correct decision region, while the correct demodulation is guaranteed by the CI constraint, which is well known [25]. Based on the SNR expression in (8), we can transform $|\overline{OA}|$ into $\left| \mathbf{h}_1^T \mathbf{w}_1 \sum_{k=1}^2 e^{j\phi_k} \right|$ then the CI constraint becomes the corresponding form in (17). \mathcal{P}_2 transforms the original “Max-SER” minimization problem into a “Min-SNR” maximization problem. By further introducing an auxiliary variable (t), \mathcal{P}_2 can be further transformed into

$$\begin{aligned} \mathcal{P}_3 : & \max_{\mathbf{w}_1, \mathbf{w}_2, t} t \\ \text{s.t. C1:} & \left\| \sum_{k=1}^2 \mathbf{w}_k e^{j(\phi_k - \phi_1)} \right\|^2 < P \\ \text{C2:} & \left| \text{Im} \left(\mathbf{h}_1^T \sum_{k=1}^2 \mathbf{w}_k e^{j(\phi_k - \phi_1)} \right) \right| \leq \\ & \left(\text{Re} \left(\mathbf{h}_1^T \sum_{k=1}^2 \mathbf{w}_k e^{j(\phi_k - \phi_1)} \right) - \right. \\ & \left. |(\mathbf{h}_1^T (\mathbf{w}_1 e^{j\phi_1} + \mathbf{w}_2 e^{j\phi_2}))| \right) \tan \theta_t \\ \text{C3:} & \text{Im}(\mathbf{h}_2^T \mathbf{w}_2) = 0, \text{Re}(\mathbf{h}_2^T \mathbf{w}_2) \geq 0 \\ \text{C4:} & |(\mathbf{h}_1^T (\mathbf{w}_1 e^{j\phi_1} + \mathbf{w}_2 e^{j\phi_2}))|^2 \geq \sigma_{u1}^2 t \\ \text{C5:} & \frac{|\mathbf{h}_2^T \mathbf{w}_2|^2}{|\mathbf{h}_2^T \mathbf{w}_1|^2 + \sigma_{u2}^2} \geq t \end{aligned} \quad (18)$$

where the auxiliary variable t represents the minimum value of the received SNR for the two CoMA users. In order to deal with the non-convex fractional constraint **C5**, we propose to transform its numerator into a concave function [37] by employing the Taylor series expansion. More specifically, **C5** is re-expressed as the following form

$$\frac{\mathcal{A}(\mathbf{w}_2)}{\mathcal{B}(\mathbf{w}_1)} \geq t, \quad (19)$$

where the expressions for $\mathcal{A}(\mathbf{w}_2)$ and $\mathcal{B}(\mathbf{w}_1)$ are given by

$$\begin{aligned} \mathcal{A}(\mathbf{w}_2) &= 2\text{Re}(\bar{\mathbf{w}}_2^H \mathbf{h}_2 \mathbf{h}_2^T \mathbf{w}_2) - \text{Re}(\bar{\mathbf{w}}_2^H \mathbf{h}_2 \mathbf{h}_2^T \bar{\mathbf{w}}_2) \\ \mathcal{B}(\mathbf{w}_1) &= |\mathbf{h}_2^T \mathbf{w}_1|^2 + \sigma_{u2}^2 \end{aligned} \quad (20)$$

where $\bar{\mathbf{w}}_2$ represents the initial feasible point of the Taylor series expansion. According to the Corollary 3 in [37], we introduce another auxiliary variable y to transform the nonconvex constraint **C5** into a convex one:

$$2y\sqrt{\mathcal{A}(\mathbf{w}_2)} - y^2\mathcal{B}(\mathbf{w}_1) \geq t, \quad (21)$$

Thus the corresponding optimization problem is further shown in (22), at the top of the page.

To solve \mathcal{P}_4 , we adopt the block coordinate ascent algorithm. Firstly, for given \mathbf{w}_1 , \mathbf{w}_2 and t , the optimal value of y^* can be obtained in a closed form as

$$y^* = \frac{\sqrt{\mathcal{A}(\mathbf{w}_2)}}{\mathcal{B}(\mathbf{w}_1)} \geq t, \quad (23)$$

Then, for given, y^* , \mathbf{w}_1 , \mathbf{w}_2 and t can be obtained via solving \mathcal{P}_4 by substituting y^* into the constraint **C5** and solve the optimization problem \mathcal{P}_5 in (24).

The alternating optimization (AO) method is employed to solve the \mathcal{P}_5 . Initially, we set the variables $\bar{\mathbf{w}}_1, \bar{\mathbf{w}}_2$, and t as zero. Subsequently, the auxiliary variable y is updated based on (23), following by updating the variables by solving

$$\begin{aligned}
 \mathcal{P}_4 : \max_{\mathbf{w}_1, \mathbf{w}_2, t, y} \quad & t \\
 \text{s.t. C1:} \quad & \left\| \sum_{k=1}^2 \mathbf{w}_k e^{j(\phi_k - \phi_1)} \right\|^2 < P \\
 \text{C2:} \quad & \left| \text{Im} \left(\mathbf{h}_1^T \sum_{k=1}^2 \mathbf{w}_k e^{j(\phi_k - \phi_1)} \right) \right| \leq \\
 & \left(\text{Re} \left(\mathbf{h}_1^T \sum_{k=1}^2 \mathbf{w}_k e^{j(\phi_k - \phi_1)} \right) - |(\mathbf{h}_1^T (\mathbf{w}_1 e^{j\phi_1} + \mathbf{w}_2 e^{j\phi_2}))| \right) \tan \theta_t \\
 \text{C3:} \quad & \text{Im}(\mathbf{h}_2^T \mathbf{w}_2) = 0, \text{Re}(\mathbf{h}_2^T \mathbf{w}_2) \geq 0 \\
 \text{C4:} \quad & 2\text{Re} \left((\bar{\mathbf{w}}_1 e^{j\phi_1} + \bar{\mathbf{w}}_2 e^{j\phi_2})^H \mathbf{h}_1 \mathbf{h}_1^T (\mathbf{w}_1 e^{j\phi_1} + \mathbf{w}_2 e^{j\phi_2}) \right) - \\
 & \text{Re} \left((\bar{\mathbf{w}}_1 e^{j\phi_1} + \bar{\mathbf{w}}_2 e^{j\phi_2})^H \mathbf{h}_1 \mathbf{h}_1^T (\bar{\mathbf{w}}_1 e^{j\phi_1} + \bar{\mathbf{w}}_2 e^{j\phi_2}) \right) \geq \sigma_{u1}^2 t \\
 \text{C5:} \quad & 2y \sqrt{\mathcal{A}(\mathbf{w}_2)} - y^2 \mathcal{B}(\mathbf{w}_1) \geq t,
 \end{aligned} \tag{22}$$

$$\begin{aligned}
 \mathcal{P}_5 : \max_{\mathbf{w}_1, \mathbf{w}_2, t} \quad & t \\
 \text{s.t. C1:} \quad & \left\| \sum_{k=1}^2 \mathbf{w}_k e^{j(\phi_k - \phi_1)} \right\|^2 < P \\
 \text{C2:} \quad & \left| \text{Im} \left(\mathbf{h}_1^T \sum_{k=1}^2 \mathbf{w}_k e^{j(\phi_k - \phi_1)} \right) \right| \leq \\
 & \left(\text{Re} \left(\mathbf{h}_1^T \sum_{k=1}^2 \mathbf{w}_k e^{j(\phi_k - \phi_1)} \right) - |(\mathbf{h}_1^T (\mathbf{w}_1 e^{j\phi_1} + \mathbf{w}_2 e^{j\phi_2}))| \right) \tan \theta_t \\
 \text{C3:} \quad & \text{Im}(\mathbf{h}_2^T \mathbf{w}_2) = 0, \text{Re}(\mathbf{h}_2^T \mathbf{w}_2) \geq 0 \\
 \text{C4:} \quad & 2\text{Re} \left((\bar{\mathbf{w}}_1 e^{j\phi_1} + \bar{\mathbf{w}}_2 e^{j\phi_2})^H \mathbf{h}_1 \mathbf{h}_1^T (\mathbf{w}_1 e^{j\phi_1} + \mathbf{w}_2 e^{j\phi_2}) \right) - \\
 & \text{Re} \left((\bar{\mathbf{w}}_1 e^{j\phi_1} + \bar{\mathbf{w}}_2 e^{j\phi_2})^H \mathbf{h}_1 \mathbf{h}_1^T (\bar{\mathbf{w}}_1 e^{j\phi_1} + \bar{\mathbf{w}}_2 e^{j\phi_2}) \right) \geq \sigma_{u1}^2 t \\
 \text{C5:} \quad & 2y^* \sqrt{\mathcal{A}(\mathbf{w}_2)} - y^{*2} \mathcal{B}(\mathbf{w}_1) \geq t,
 \end{aligned} \tag{24}$$

the \mathcal{P}_5 with CVX tool. By iterating through these steps, the algorithm can converge within a limited number of iterations. For clarity, we summarize the algorithm in Algorithm 2 below.

1) Convergence analysis

The AO method is used to solve our proposed problem \mathcal{P}_5 , where the variables are updated iteratively. The convergence of the proposed AO algorithms can be guaranteed for following two reasons: 1) Within each iteration of the proposed AO algorithm, the value of the objective function monotonically increases. This property ensures progress towards a better solution in each iteration, leading to convergence [38]. 2) The objective function value has an upper bound for the proposed problem, which is determined

by the CI constraint and SNR constraint. This upper bound acts as a convergence criterion, ensuring that the optimization process does not diverge and remains within a feasible range [39].

2) Optimality analysis

The \mathcal{P}_5 is transformed from \mathcal{P}_1 , during the derivation, the Taylor series expansion is used to transform the original non convex SNR constraint into convex, which makes the solution of \mathcal{P}_5 is sub-optimal.

B. Review: Conventional NOMA Precoding

Similarly, in order to minimize the SER of conventional NOMA scheme, we can consider the following optimization problem:

Algorithm 2 Block Coordinate Ascent Algorithm for solving \mathcal{P}_5 .

Initialization : $\bar{\mathbf{w}}_1 = 0, \bar{\mathbf{w}}_2 = 0, t = 0$

Repeat

Update y based on (23);

Update $\mathbf{w}_1, \mathbf{w}_2$ and t by solving \mathcal{P}_5

Until Convergence

$$\begin{aligned} \mathcal{P}_1 : & \max_{\mathbf{w}_1, \mathbf{w}_2} \min_k \{ \text{SNR}_k \} \\ \text{s.t. } & \mathbf{C1}: \|\mathbf{w}_1\|^2 + \|\mathbf{w}_2\|^2 \leq P \\ & \mathbf{C2}: \gamma_{x_2 \rightarrow u_1} \geq r_2 \end{aligned} \quad (25)$$

The constraint **C2** to ensure the successful SIC for the strong user. To deal with the non-convex objective function, an auxiliary variable t is introduced to equivalently convert the original problem \mathcal{P}_1 into a new problem as follows

$$\begin{aligned} \mathcal{P}_2 : & \max_{\mathbf{w}_1, \mathbf{w}_2, t} t \\ \text{s.t. } & \mathbf{C1}: \|\mathbf{w}_1\|^2 + \|\mathbf{w}_2\|^2 \leq P \\ & \mathbf{C2}: |\mathbf{h}_1^T \mathbf{w}_2|^2 \geq (|\mathbf{h}_1^T \mathbf{w}_1|^2 + \sigma_{u_1}^2) r_2 \\ & \mathbf{C3}: |\mathbf{h}_2^T \mathbf{w}_2|^2 \geq t |\mathbf{h}_2^T \mathbf{w}_1|^2 + t \sigma_{u_2}^2 \end{aligned} \quad (26)$$

Note that the objective function and the constraint **C1** in \mathcal{P}_2 are convex, and the challenge is only in the constraints **C2** and **C3**. However, we would like to mention that, similar problem has been considered and solved in the literature using bisection-based method, we refer the reader to [40]–[43] for more details.

VI. Receiver Complexity

In this section we focus our attention on the receiver complexity, which impacts the user equipment where the computational resources are scarce. To compare the computational receiver complexity of CoMA with conventional NOMA, we provide here the complexity analysis for the detection process. In the complexity analysis, the number of complex operations is used as the complexity metric. The complexity of SIC can be divided into two parts: decoding and subtraction.

For classical NOMA, the weak user needs to detect its signal, while the powerful user, first detects the weak user's signal, then subtracts it from the received signal, before finally detecting its own signal. Assuming an ML detector, the complexity of NOMA for pair k can be obtained as [44], [45]

$$\begin{aligned} \mathcal{C}_{NOMA-pair,k} = & \sum_{i=1}^2 \underbrace{(4NM_k + 2M_k^N)}_{ML \text{ detection}} \times (2 - i + 1) \\ & + \underbrace{\mathcal{O}(M_k^2)}_{\text{Subtraction}} \end{aligned} \quad (27)$$

where M_k is the modulation order of pair k . The total complexity of NOMA for all pairs can be written as

$$\begin{aligned} \mathcal{C}_{NOMA} = & \sum_{k=1}^K \left(\sum_{i=1}^2 \underbrace{(4NM_k + 2M_k^N)}_{ML \text{ detection}} \times (2 - i + 1) \right. \\ & \left. + \underbrace{\mathcal{O}(M_k^2)}_{\text{Subtraction}} \right) \end{aligned} \quad (28)$$

where K is number of pairs.

On the other hand, for CoMA, the weak user needs to apply classical detection for its signal, while the powerful user detects its signal without the need to remove the interference. Accordingly, the complexity of CoMA for pair k can be written as [44], [45]

$$\mathcal{C}_{CI-NOMA-pair,k} = \underbrace{(4NM_k + 2M_k^N)}_{ML \text{ detection}} + \underbrace{D_k(M_k)}_{CI \text{ detection}} \quad (29)$$

where $D_k(M_k)$ is the complexity of decision operation upon the received signal for pair k which depends on the modulation order. The total complexity of CoMA for all pairs can be obtained as

$$\mathcal{C}_{CI-NOMA} = \sum_{k=1}^K \left(\underbrace{(4NM_k + 2M_k^N)}_{ML \text{ detection}} + \underbrace{D_k(M_k)}_{CI \text{ detection}} \right). \quad (30)$$

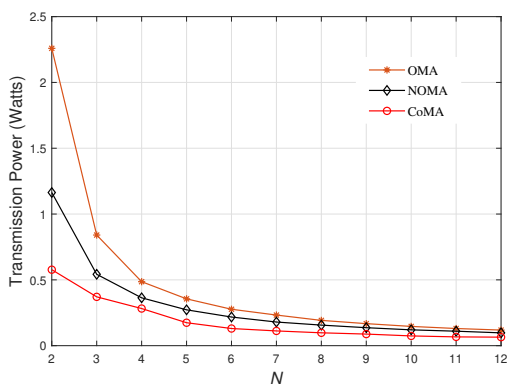
VII. Numerical Results

To evaluate the performance of the proposed CoMA technique, in this Section several numerical results for CoMA are presented and compared with conventional NOMA and OMA using Monte Carlo simulations. In these results we assume the users have same noise variance, $\sigma_{u_1}^2 = \sigma_{u_2}^2 = \sigma^2$. The optimal precoders for OMA have been obtained by solving optimization problems as in [4].

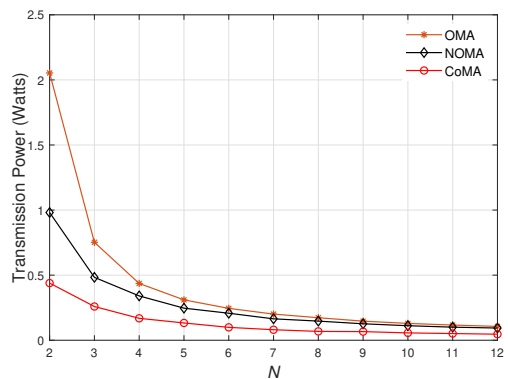
The simulation algorithm is composed of the following steps.

1-Define System Parameters: Identify and specify the key system parameters.

2-Setup the Simulation Loop: Create a loop that will run the simulation multiple times to capture the effects of randomness. The number of iterations will depend on the desired level of statistical significance.

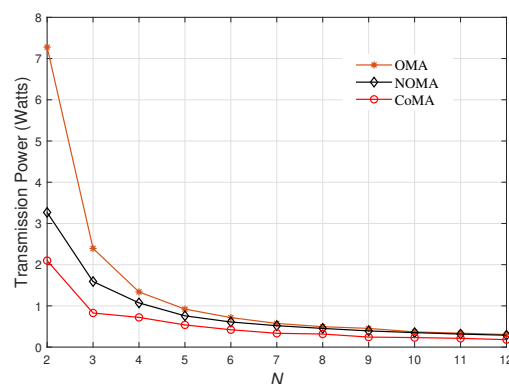


(a) Power consumption versus number of BS antennas when $(r_1, r_2, \sigma_1, \sigma_2) = (1, 1, 2, 1)$.

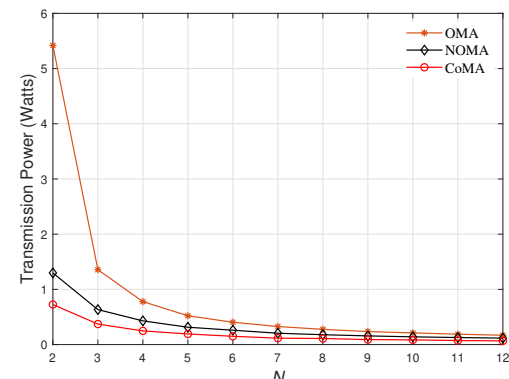


(b) Power consumption versus number of BS antennas when $(r_1, r_2, \sigma_1, \sigma_2) = (1, 1, 3, 1)$.

FIGURE 6. Power consumption for OMA, NOMA and CoMA versus number of BS antennas for different channel variance.



(a) Power consumption versus number of BS antennas when $(r_1, r_2, \sigma_1, \sigma_2) = (1, 3, 2, 1)$.



(b) Power consumption versus number of BS antennas when $(r_1, r_2, \sigma_1, \sigma_2) = (3, 1, 2, 1)$.

FIGURE 7. Power consumption for OMA, NOMA and CoMA versus number of BS antennas for different target rates.

3-Generate Random Variables: Use MATLAB functions to generate random values for the random variables in the system.

4- Apply Algorithm 1 to evaluate the power minimization and Algorithm 2 for the SER minimization.

5-Collect and Store Results: After each iteration of the simulation, collect and store the results in the initialized variables.

6-Aggregate Results: After completing all iterations, aggregate the results to analyze the overall system performance.

7-Visualization: Create plots to represent the results.

To measure the performance of CoMA technique in terms of total power consumption for MU-MISO systems, in Fig. 6 we plot the power consumption versus number of BS antennas N for OMA, conventional NOMA and CoMA with QPSK signaling using the power minimization approaches in (15), and (13). The case when $(r_1, r_2, \sigma_1, \sigma_2) = (1, 1, 2, 1)$ is presented in Fig. 6a and when $(r_1, r_2, \sigma_1, \sigma_2) = (1, 1, 3, 1)$ is shown in Fig.6b. Several observations can be extracted from these results. Firstly it can be observed that, CoMA scheme has a significant enhancement in terms of power consumption in comparison with the conventional NOMA

and OMA schemes. It is also noted that the proposed CoMA scheme yields a significant performance gain in the symmetric scenario when $N = 2$. On the other hand, it is worth pointing out that the difference between the considered schemes becomes negligible when N is large. Nevertheless, the complexity gains of CoMA by removing the SIC operation persist. In addition, the total transmission power decreases when the channel variance of user 1 increases or if there is a notable disparity of channel strengths among users, as shown in Figs. 6a and 6b. This is because the strong user, user 1, in this case needs small power to achieve its target rate, r_1 .

Furthermore, Fig. 7 shows the power consumption for OMA, NOMA and CoMA versus number of BS antennas for different target rates. Fig. 7a presents the case when $(r_1, r_2, \sigma_1, \sigma_2) = (1, 3, 2, 1)$ while Fig. 7b shows the case when $(r_1, r_2, \sigma_1, \sigma_2) = (3, 1, 2, 1)$. It can be clearly seen in these results that, increasing the target rates of the two users leads to boost the transmission power, and this increasing in the power is essential when the target rate of the second user, r_2 , is higher.

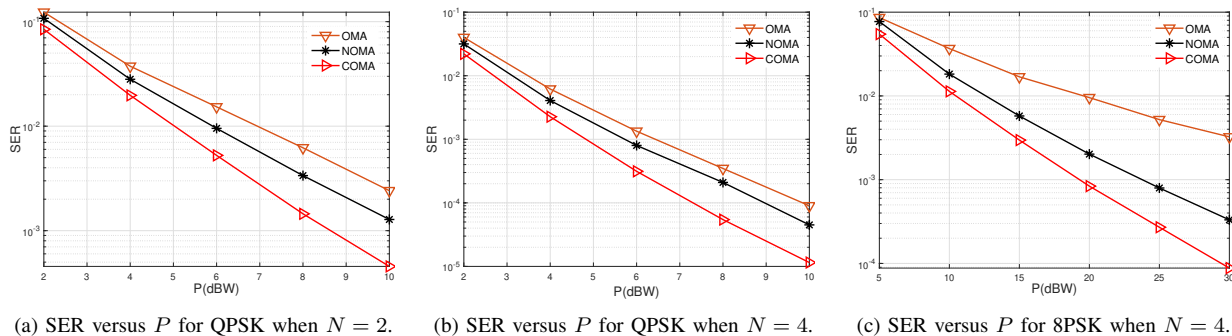


FIGURE 9. SER for OMA, NOMA and CoMA versus P for different number of antennas and modulation order.

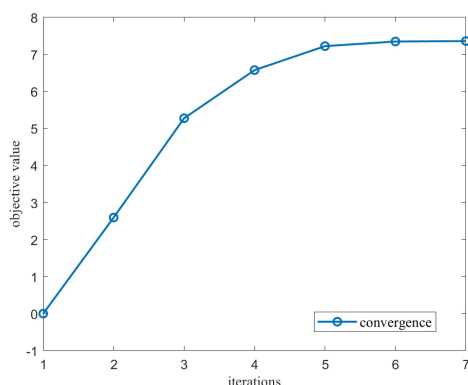


FIGURE 8. Convergence of Algorithm 2.

Fig. 8 depicts the convergence of the Algorithm 2, it can be seen that the algorithm converges within a few iterations, underscoring the effectiveness of the proposed method.

To evaluate the error rate performance of the proposed CoMA scheme, Fig. 9 illustrates the SER versus the total transmit power, P , for OMA, conventional NOMA and CoMA with different values of number of BS antennas and modulation order. Fig. 9a and Fig. 9b show the SER versus the total transmit power when $N = 2$ and $N = 4$, respectively, for QPSK, while Fig. 9c represents the SER versus the transmit power when $N = 4$ for 8PSK scheme. Several interesting features can be noted in this figure. Firstly, it is evident from these results that the SER reduces with increasing the transmit power, and CoMA scheme always outperforms OMA and conventional NOMA techniques in the all power levels. Looking closer at Fig. 9a and Fig. 9b we can observe that, increasing number of BS antennas reduces the SER, and the gain attained by CoMA over conventional NOMA is almost fixed with the transmit power. Finally, from Fig. 9b and Fig. 9c it is clear that CoMA has better performance than the other two schemes and this superiority is major when the total transmit power is high.

The computational receiver complexity of CoMA and conventional NOMA versus number of BS antennas N

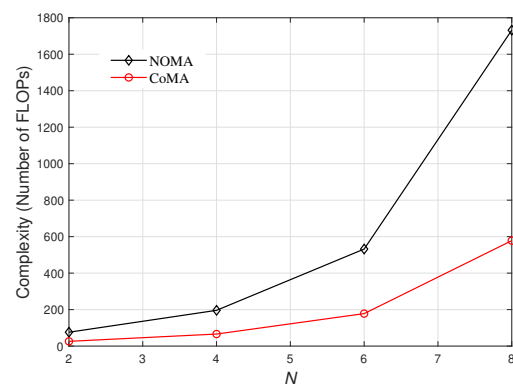


FIGURE 10. Computational complexity versus number of BS antennas for BPSK.

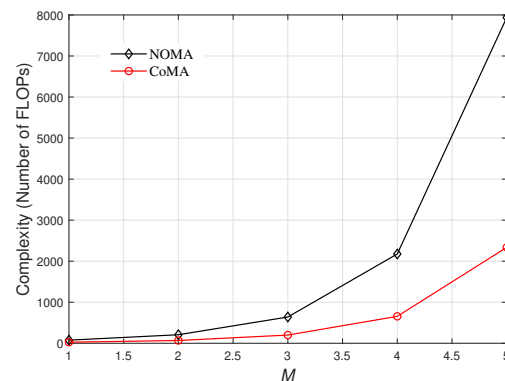


FIGURE 11. Computational complexity versus modulation order.

is presented in Fig. 10. It can be observed from these results that, CoMA substantially reduces the computational complexity, which is desirable in hardware-limited networks. In addition, the computational complexity gap between the two schemes is much wider when number of BS antennas N is high.

Finally, Fig. 11 shows the computational receiver complexity of CoMA and conventional NOMA versus the modulation order M when $N = 2$. As shown in the figure, conventional NOMA scheme has higher computational complexity than CoMA. In addition, the

conventional NOMA becomes computationally expensive for higher modulation orders.

VIII. Conclusions

In this paper a CoMA scheme for user pairing NOMA systems was proposed and investigated. Firstly, for a given pair of users, the minimum transmission power and the optimal precoding vectors of CoMA scheme has been obtained. Then, optimal precoding vectors that minimizing the symbol error rate subject to total power constrains for CoMA scheme has been considered. Further, the complexity of CoMA has been studied and compared with conventional NOMA scheme in terms of the total number of complex operations. Simulation results have been provided to show that, CoMA scheme consumes much less power than conventional NOMA and OMA schemes to achieve similar target rates. In addition, CoMA scheme produces lower error rate than conventional NOMA technique over the all transmit power values. Furthermore, the proposed CoMA scheme implicates very low computational receiver complexity compared to conventional NOMA technique.

REFERENCES

- [1] Z. Ding, Y. Liu, J. Choi, Q. Sun, M. Elkashlan, C. L. I, and H. V. Poor, "Application of non-orthogonal multiple access in LTE and 5G networks," *IEEE Commun. Mag.*, vol. 55, no. 2, pp. 185–191, Feb. 2017.
- [2] Z. Ding, Z. Yang, P. Fan, and H. V. Poor, "On the performance of non-orthogonal multiple access in 5G systems with randomly deployed users," *IEEE Signal Processing Letters*, vol. 21, no. 12, pp. 1501–1505, Dec. 2014.
- [3] Z. Yang, Z. Ding, P. Fan, and G. K. Karagiannidis, "On the performance of non-orthogonal multiple access systems with partial channel information," *IEEE Trans. Commun.*, vol. 64, no. 2, pp. 654–667, Feb. 2016.
- [4] Z. Chen, Z. Ding, P. Xu, and X. Dai, "Optimal precoding for a QoS optimization problem in two-user MISO-NOMA downlink," *IEEE Communications Letters*, vol. 20, no. 6, pp. 1263–1266, 2016.
- [5] S. Timotheou and I. Krikidis, "Fairness for non-orthogonal multiple access in 5G systems," *IEEE Signal Processing Letters*, vol. 22, no. 10, pp. 1647–1651, 2015.
- [6] L. Zhang, J. Liu, M. Xiao, G. Wu, Y. C. Liang, and S. Li, "Performance analysis and optimization in downlink NOMA systems with cooperative full-duplex relaying," *IEEE Journal on Selected Areas in Communications*, vol. 35, no. 10, pp. 2398–2412, Oct. 2017.
- [7] Z. Ding, P. Fan, and H. V. Poor, "Impact of user pairing on 5G non-orthogonal multiple-access downlink transmissions," *IEEE Transactions on Vehicular Technology*, vol. 65, no. 8, pp. 6010–6023, Aug. 2016.
- [8] M. Zeng, A. Yadav, O. A. Dobre, G. I. Tsiropoulos, and H. V. Poor, "On the sum rate of MIMO-NOMA and MIMO-OMA systems," *IEEE Wireless Communications Letters*, vol. 6, no. 4, pp. 534–537, 2017.
- [9] L. Shi, B. Li, and H. Chen, "Pairing and power allocation for downlink nonorthogonal multiple access systems," *IEEE Transactions on Vehicular Technology*, vol. 66, no. 11, pp. 10084–10091, 2017.
- [10] C. Masouros and E. Alsusa, "Dynamic linear precoding for the exploitation of known interference in MIMO broadcast systems," *IEEE Transactions on Wireless Communications*, vol. 8, no. 3, pp. 1396–1404, March 2009.
- [11] C. Masouros, M. Sellathurai, and T. Ratnarajah, "Vector perturbation based on symbol scaling for limited feedback MISO downlinks," *IEEE Transactions on Signal Processing*, vol. 62, no. 3, pp. 562–571, Feb 2014.
- [12] C. Masouros and G. Zheng, "Exploiting known interference as green signal power for downlink beamforming optimization," *IEEE Transactions on Signal Processing*, vol. 63, no. 14, pp. 3628–3640, July 2015.
- [13] M. Alodeh, S. Chatzinotas, and B. r. Ottersten, "Constructive multiuser interference in symbol level precoding for the MISO downlink channel," *IEEE Transactions on Signal Processing*, vol. 63, no. 9, pp. 2239–2252, 2015.
- [14] A. Haqiqatnejad, F. Kayhan, and B. Ottersten, "Symbol-level precoding design based on distance preserving constructive interference regions," *IEEE Transactions on Signal Processing*, vol. 66, no. 22, pp. 5817–5832, Nov 2018.
- [15] —, "Constructive interference for generic constellations," *IEEE Signal Processing Letters*, vol. 25, no. 4, pp. 586–590, April 2018.
- [16] R. de Miguel and R. R. Muller, "On convex vector precoding for multiuser MIMO broadcast channels," *IEEE Transactions on Signal Processing*, vol. 57, no. 11, pp. 4497–4508, 2009.
- [17] R. R. Muller, D. Guo, and A. L. Moustakas, "Vector precoding for wireless MIMO systems and its replica analysis," *IEEE Journal on Selected Areas in Communications*, vol. 26, no. 3, pp. 530–540, 2008.
- [18] S. Timotheou, G. Zheng, C. Masouros, and I. Krikidis, "Exploiting constructive interference for simultaneous wireless information and power transfer in multiuser downlink systems," *IEEE Journal on Selected Areas in Communications*, vol. 34, no. 5, pp. 1772–1784, May 2016.
- [19] Y. Choi, J. Lee, M. Rim, and C. G. Kang, "Constructive interference optimization for data-aided precoding in multi-user miso systems," *IEEE Transactions on Wireless Communications*, vol. 18, no. 2, pp. 1128–1141, 2019.
- [20] D. Spano, M. Alodeh, S. Chatzinotas, and B. Ottersten, "Symbol-level precoding for the nonlinear multiuser miso downlink channel," *IEEE Transactions on Signal Processing*, vol. 66, no. 5, pp. 1331–1345, 2018.
- [21] A. Haqiqatnejad, F. Kayhan, and B. Ottersten, "Robust sinr-constrained symbol-level multiuser precoding with imperfect channel knowledge," *IEEE Transactions on Signal Processing*, vol. 68, pp. 1837–1852, 2020.
- [22] A. Li and C. Masouros, "Interference exploitation precoding made practical: Optimal closed-form solutions for PSK modulations," *IEEE Transactions on Wireless Communications*, pp. 1–1, 2018.
- [23] A. Li, C. Masouros, B. Vucetic, Y. Li, and A. L. Swindlehurst, "Interference exploitation precoding for multi-level modulations: Closed-form solutions," *IEEE Transactions on Communications*, vol. 69, no. 1, pp. 291–308, 2021.
- [24] A. Salem, C. Masouros, and K. Wong, "Sum rate and fairness analysis for the MU-MIMO downlink under PSK signalling: Interference suppression vs exploitation," *IEEE Transactions on Communications*, pp. 1–1, 2019.
- [25] A. Li, D. Spano, J. Krivochiza, S. Domouchtsidis, C. G. Tsinos, C. Masouros, S. Chatzinotas, Y. Li, B. Vucetic, and B. Ottersten, "A tutorial on interference exploitation via symbol-level precoding: Overview, state-of-the-art and future directions," *IEEE Communications Surveys Tutorials*, vol. 22, no. 2, pp. 796–839, 2020.
- [26] S.-L. Shieh and Y.-C. Huang, "A simple scheme for realizing the promised gains of downlink nonorthogonal multiple access," *IEEE Transactions on Communications*, vol. 64, no. 4, pp. 1624–1635, 2016.
- [27] M. Qiu, Y.-C. Huang, S.-L. Shieh, and J. Yuan, "A lattice-partition framework of downlink non-orthogonal multiple access without SIC," *IEEE Transactions on Communications*, vol. 66, no. 6, pp. 2532–2546, 2018.
- [28] M. Qiu, Y.-C. Huang, J. Yuan, and C.-L. Wang, "Lattice-partition-based downlink non-orthogonal multiple access without SIC for slow fading channels," *IEEE Transactions on Communications*, vol. 67, no. 2, pp. 1166–1181, 2019.
- [29] K. Chung, "Correlated superposition coding: Lossless two-user NOMA implementation without SIC under user-fairness," *IEEE Wireless Communications Letters*, vol. 10, no. 9, pp. 1999–2003, 2021.
- [30] A. Salem and C. Masouros, "Noma made practical: Removing the sic through constructive interference," in *2022 International Symposium on Wireless Communication Systems (ISWCS)*, 2022, pp. 1–6.
- [31] M. Vaezi, R. Schober, Z. Ding, and H. V. Poor, "Non-orthogonal multiple access: Common myths and critical questions," *IEEE Wireless Communications*, vol. 26, no. 5, pp. 174–180, 2019.
- [32] D. N. C. Tse and P. Viswanath, *Fundamentals of Wireless Communication*. Cambridge University Press-Cambridge, 2005.

- [33] B. Clerckx, Y. Mao, R. Schober, E. A. Jorswieck, D. J. Love, J. Yuan, L. Hanzo, G. Y. Li, E. G. Larsson, and G. Caire, "Is NOMA efficient in multi-antenna networks? a critical look at next generation multiple access techniques," *IEEE Open Journal of the Communications Society*, vol. 2, pp. 1310–1343, 2021.
- [34] Y. Mao, O. Dizdar, B. Clerckx, R. Schober, P. Popovski, and H. V. Poor, "Rate-splitting multiple access: Fundamentals, survey, and future research trends," *IEEE Communications Surveys and Tutorials*, vol. 24, no. 4, pp. 2073–2126, 2022.
- [35] Z.-q. Luo, W.-k. Ma, A. M.-c. So, Y. Ye, and S. Zhang, "Semidefinite relaxation of quadratic optimization problems," *IEEE Signal Processing Magazine*, vol. 27, no. 3, pp. 20–34, 2010.
- [36] J. Xu, L. Liu, and R. Zhang, "Multiuser MISO beamforming for simultaneous wireless information and power transfer," *IEEE Transactions on Signal Processing*, vol. 62, no. 18, pp. 4798–4810, 2014.
- [37] K. Shen and W. Yu, "Fractional programming for communication systems part I: Power control and beamforming," *IEEE Transactions on Signal Processing*, vol. 66, no. 10, pp. 2616–2630, 2018.
- [38] Q. Li, M. Hong, H.-T. Wai, Y.-F. Liu, W.-K. Ma, and Z.-Q. Luo, "Transmit solutions for MIMO wiretap channels using alternating optimization," *IEEE Journal on Selected Areas in Communications*, vol. 31, no. 9, pp. 1714–1727, 2013.
- [39] A. A. Salem, M. H. Ismail, and A. S. Ibrahim, "Active reconfigurable intelligent surface-assisted MISO integrated sensing and communication systems for secure operation," *IEEE Transactions on Vehicular Technology*, vol. 72, no. 4, pp. 4919–4931, 2023.
- [40] S. Timotheou and I. Krikidis, "Fairness for non-orthogonal multiple access in 5G systems," *IEEE Signal Processing Letters*, vol. 22, no. 10, pp. 1647–1651, 2015.
- [41] R. Jiao, L. Dai, W. Wang, F. Lyu, N. Cheng, and X. Shen, "Max-min fairness for beamspace MIMO-NOMA: From single-beam to multi-beam," *IEEE Transactions on Wireless Communications*, vol. 21, no. 2, pp. 739–752, 2022.
- [42] R. Jiao and L. Dai, "On the max-min fairness of beamspace MIMO-NOMA," *IEEE Transactions on Signal Processing*, vol. 68, pp. 4919–4932, 2020.
- [43] A. Z. Yalcin, M. K. Cetin, and M. Yuksel, "Max-min fair precoder design and power allocation for MU-MIMO NOMA," *IEEE Transactions on Vehicular Technology*, vol. 70, no. 6, pp. 6217–6221, 2021.
- [44] J. W. Kim, S. Y. Shin, and V. C. M. Leung, "Performance enhancement of downlink NOMA by combination with GSSK," *IEEE Wireless Communications Letters*, vol. 7, no. 5, pp. 860–863, 2018.
- [45] F. Kara and H. Kaya, "Performance analysis of SSK-NOMA," *IEEE Transactions on Vehicular Technology*, vol. 68, no. 7, pp. 6231–6242, 2019.